Monatshefte für Chemie 139, 7–11 (2008)
DOI 10.1007/s00706-007-0728-9
Printed in The Netherlands

Monatshefte für Chemie
Chemical Monthly

The Photocatalytic Degradation of Imazapyr

Josy Anteveli Osajima[1], **Hamilton M. Ishiki**[2], and **Keiko Takashima**[1,*]

[1] Departamento de Química, CCE, Universidade Estadual de Londrina, Londrina, PR, Brazil
[2] Faculdade de Farmácia e Bioquímica, Universidade do Oeste Paulista, Presidente Prudente, SP, Brazil

Received February 28, 2007; accepted (revised) May 23, 2007; published online July 23, 2007

Summary. The degradation of imazapyr, an imidazolinone herbicide, in aqueous solution has been investigated with TiO_2 slurry as photocatalyst at 30°C under UV radiation. The depletion of imazapyr concentration in an aqueous suspension followed 1st order kinetic behavior. The influence of *pH* and the charge densities of imazapyr geometries were calculated at the semi-empirical AM1 level, and the effect of temperature was investigated. The addition of electron acceptors such as potassium persulfate and hydrogen peroxide showed that the rate constant doubled at least. At higher persulfate concentrations the herbicide degradation was more efficient in direct photolysis than TiO_2-photocatalysis. The degradation rate constant increased by 38% upon variation of the temperature between 20.0 and 50.0°C and displayed non-*Arrhenius* behavior.

Keywords. Photodegradation; Titanium dioxide; Herbicide; Oxidant.

Introduction

Purification of contaminated water by pesticide wastes and industrial effluents may be carried out by a combination of procedures, such as flocculation, filtration, sterilization, and chemical oxidation. After filtration and elimination of particles in suspension, biological treatment is the ideal process. Advanced Oxidation Processes (AOPs) have emerged as an attractive alternative for the treatment of pesticide wastes that are refractory to physico-chemical and biological systems. These processes are based on the generation of the hydroxyl radical ($HO^{\bullet}$) as reactive species, characterized by its small selectivity upon attack [1, 2]. Among the AOPs, heterogeneous photocatalysis is based on the irradiation of an n-type semiconductor such as TiO_2 with a band-gap energy of 3.2 eV. Under these conditions, an electron may be promoted from the valence band to the conduction band (e^-_{cb}), leaving behind an electron vacancy or hole in the valence band (h^+_{vb}). This process generates oxidative and reductive sites that catalyze chemical reactions, oxidize organic compounds, and reduce dissolved metallic ions [2]. On the other hand, there is an energy-wasting step that takes place by electron-hole recombination which leads to low quantum yield. This can be avoided by adding electron acceptors such as hydrogen peroxide, persulfate ion, periodate ion, *etc.* to the photocatalytic system [3–8]. These species can scavenge the excited electron and reduce to hydroxyl radical, enhancing the photocatalytic degradation of pollutants.

Imidazolinone herbicides have been used on a large scale as plant growth regulator for agricultural purposes. Among these compounds, imazapyr is a non-selective herbicide for control of weeds including annual and perennial grasses and broadleaved herbs, as well as woody species. Imazapyr has no aquatic use; however, it could potentially enter in the surface water by spray drift during application or runoff after application. It persists in soil for over a year, and persistence studies suggest that residues damage plants at very low concentrations. Since imazapyr is a weak acid herbicide, environmental *pH* will determine its chemical structure, which in turn, determines its environmental persistence and mobility [9]. *Pizarro et al.*

* Corresponding author. E-mail: keiko@uel.br

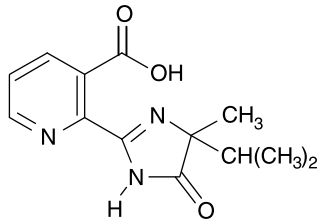

Fig. 1. Structural formula of imazapyr ($C_{13}H_{15}N_3O_3$; 2-[4,5-dihydro-4-methyl-4-(1-methylethyl)-5-oxo-1*H*-imidazol-2-yl]-3-pyridinecarboxylic acid)

[10] investigated imazapyr degradation using two TiO_2 types (Degussa P-25 and Millennium P-500) in an open vessel, illuminated with an irradiance of $4.9\,mW\,cm^{-2}$. Some operational parameters were compared for two TiO_2 types in suspension. *Carrier et al.* [11] continued this study by varying other parameters, such as the influence of *pH*, the radiant flux of the irradiation source, the effect of copper and nickel amount, and they proposed the photocatalytic mechanism for this system. In the last two decades, concerning photocatalysis, several hundred investigations [1, 2, 12–14] have been carried out as the reaction rate on TiO_2 surface depends on various parameters: reactor geometry, nature and concentrations of substrate, semiconductor, and oxidant, light intensity, temperature, *pH* value, and the presence of competitive interfering species. In this paper, we present the study of some operational parameters not yet investigated for imazapyr (Fig. 1) providing the determination of partial atomic charge in order to understand the variation of the degradation rate constant as a function of *pH*. Furthermore, the addition of the oxidants such as hydrogen peroxide and potassium persulfate, and the effect of temperature were investigated using Degussa P-25 TiO_2 in aqueous suspension under artificial illumination with a lower irradiance [$(420 \pm 19)\ \mu W\,cm^{-2}$].

Results and Discussion

Effect of pH Value

The effect of *pH* variation was investigated from 3.0 up to 11.0 at 30.0°C. The *pH* was adjusted through the addition of suitable amounts of $0.10\,mol\,dm^{-3}$ NaOH and/or $0.10\,mol\,dm^{-3}$ HCl. The degradation rate for imazapyr as function of *pH* is shown in Fig. 2. The rate constant varied from $2.45 \times 10^{-3}\,min^{-1}$ at *pH* 3, attained the maximum value of $3.03 \times 10^{-2}\,min^{-1}$ at *pH* 4.0, and decreased up to $4.8 \times 10^{-3}\,min^{-1}$ at *pH* 10.0. The effect of *pH* may be largely explained by the interaction between the surface charge of TiO_2 and the ionizable functional groups of herbicide. The bifunctional imazapyr has pK_{a1} of 1.9 corresponding to the amino group and pK_{a2} of 3.8 to the carboxylic acid [16]. Consequently, these species may be in the protonated form (imp^+) at $pH \leq 1.9$, zero charged ($imp^{\pm}$) at *pH* 2.85, or yet, with negative charge (imp^-) at $pH \geq 3.8$. The zero point charge of TiO_2 (P-25) is approximately at *pH* 6.3, as TiOH [17]. This means that TiO_2 surface displays a positive charge ($TiOH_2^+$) at lower *pH* than this value, and is negatively charged (TiO^-) at higher *pH* [17]. From the above information it may be concluded that two different imazapyr species could react with the photocatalyst. The largest rate constant ($3.03 \times 10^{-2}\,min^{-1}$) occurs when imazapyr is adsorbed as imp^- over $TiOH_2^+$ at *pH* 4.0 by electrostatic attraction. Conversely, the rate constant at *pH* 3.0 is smaller ($2.45 \times 10^{-2}\,min^{-1}$), because the adsorption would predominantly take place as a zero charge species. The decrease in the rate constant at higher *pH* is attributed to the repulsion between the negatively charged herbicide and TiOH or TiO^-.

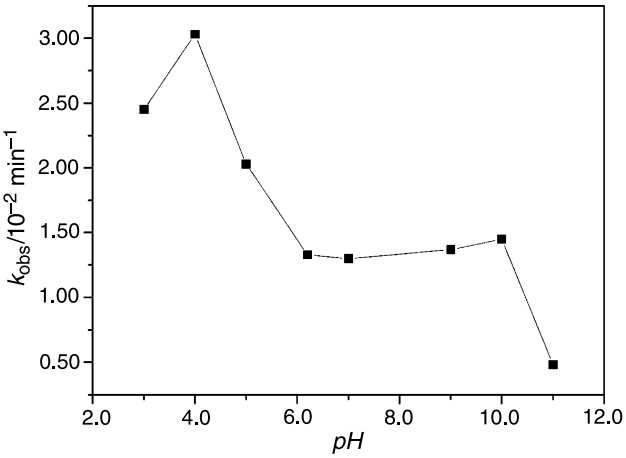

Fig. 2. Rate constant of imazapyr degradation over TiO_2 ($5.0\,g\,dm^{-3}$) as a function of *pH* at 30.0°C

In order to understand the variation of the degradation rate constant as a function of *pH*, the partial atomic charges of the imazapyr molecule were calculated along with heats of formation for the imp^+, $imp^{\pm}$, and imp^- species. The atomic charges corresponding to the heteroatoms are presented in Table 1. From this table the oxygen atom presented the most negative charge densities among the imazapyr

Table 1. Partial atomic charges of protonated (imp^+), zero charge ($imp^\pm$), and deprotonated (imp^-) species of imazapyr heteroatoms

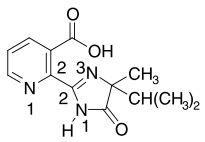

Heteroatom	Charge density		
	imp^+	$imp^\pm$	imp^-
N1 (pyridine)	−0.108	−0.135	−0.120
N3	−0.025	−0.183	−0.201
N1	−0.149	−0.360	−0.345
O (hydroxyl)	−0.267	−0.303	−0.567
O (carbonyl)	−0.425	−0.339	−0.522
O (oxo)	−0.134	−0.309	−0.351

species. For instance, the charge densities at imp^- on hydroxyl and carbonyl of the carboxylic group were, −0.567 and −0.522, meanwhile in imidazolyl group displayed −0.351. Also, the charge density on N3 nitrogen of the imidazolyl ring is more negative (−0.201) at imp^-. Conversely, the N1 nitrogen corresponding to the pyridinic (−0.135) and imidazolyl (−0.360) rings were more negative at $imp^\pm$. The heats of formation for the optimized geometries of imp^-, $imp^\pm$, and imp^+ species were estimated as −397.39, −258.62, and 438.27 kJ mol^{-1}. This means that the $imp^\pm$ dihedral angle equivalent to N3(imidazol)-C2(imidazol)-C2(pyridine)-N1(pyridine) was estimated as being 212°. For this reason, we supposed that the adsorption of this species has occurred through the carboxylic oxygen positioned at a reasonable distance (6.98 Å) from the oxo group. As a consequence, the herbicide adsorption on TiO_2 was not very favorable at *pH* 3.0, justifying the lowest rate constant of 2.45×10^{-2} min^{-1}. On the other hand, the N3(imidazol)-C2(imidazol)-C2(pyridine)-N1(pyridine) dihedral angle for imp^- was calculated as being 312°. In this case the large negative charge density due to the relatively small distance (4.48 Å) between the oxygen atoms, has favored the imazapyr (imp^-) adsorption on the TiO_2 surface as $TiOH_2^+$. Therefore, this condition has led to establish the largest rate constant (3.03×10^{-2} min^{-1}) at *pH* 4.0. The rate constant decreased at higher *pH*, where k_{obs} was 2.03×10^{-2} min^{-1} at *pH* 5 and attributed to the less positive charge density of TiO_2 in the nearly zero charge *pH* (6.3). This effect became more evident, due to the predominance of the TiO^- species in the *pH* range from 6.2 to 10.0. These data demonstrate that the approximation of imazapyr molecule becomes less favorable inhibiting the herbicide adsorption on the TiO_2 surface due to the electrostatic repulsion, decreasing the rate constant to 0.48×10^{-2} min^{-1} [18].

Effect of Electron Acceptors

The effect of persulfate addition on the degradation rate constant was investigated by varying persulfate concentrations from 0.10×10^{-2} to 50.0×10^{-2} mol dm^{-3} in aqueous solution and in TiO_2 suspension at *pH* = 4.0 and 30.0°C under UV irradiation as displayed in Table 2. We observed a linear behavior from 0.10×10^{-2} up to 5.0×10^{-2} mol dm^{-3} $S_2O_8^{2-}$ in both cases. The rate constants were equal to 0.36×10^{-2} and 5.94×10^{-2} min^{-1} in persulfate medium ($UV/S_2O_8^{2-}$) with a slope of 1.13 mol dm^{-3} min^{-1} ($r = 0.9977$), while in TiO_2 suspension ($UV/S_2O_8^{2-}/TiO_2$) the rate constants were equal to 2.20×10^{-2} and 11.1×10^{-2} min^{-1} with a slope of 0.40 mol dm^{-3} min^{-1} ($r = 0.9991$). This analogous behavior until this concentration could be justified in terms of the sulfate radical anion, $SO_4^{\bullet -}$, generation, a very strong oxidizing agent, by thermal and photolytic conditions for $\lambda < 270$ nm (Eq. (1)). Furthermore, the rate constant enhancement may be due to the production of hydroxyl radical (Eq. (2)) and molecular oxygen

Table 2. Effects of oxidants on the degradation rate constant of imazapyr under photolysis and TiO_2-photocatalysis at 30.0°C

$[S_2O_8^{2-}]$ 10^2/mol dm^{-3}	$[H_2O_2]$ 10^2/mol dm^{-3}	k_{obs} 10^2/min^{-1}	
		Direct photolysis	TiO_2-photocatalysis
0.10	–	0.36	2.20
1.0	–	1.34	3.30
2.5	–	2.75	6.26
5.0	–	5.94	11.1
20.0	–	12.6	16.3
50.0	–	23.9	7.06
–	1.0	0.41	2.15
–	2.5	0.48	2.00
–	5.0	0.51	5.56
–	7.5	0.53	1.93
–	10.0	0.59	1.18

(Eq. (3)) from the reaction between $SO_4^{\bullet -}$ and H_2O [3–6, 8]:

$$S_2O_8^{2-} + e^-_{aq} \rightarrow SO_4^{\bullet -} + SO_4^{2-} \quad (1)$$

$$SO_4^{\bullet -} + H_2O \rightarrow HO^{\bullet} + SO_4^{2-} + H^+ \quad (2)$$

$$4SO_4^{\bullet -} + 2H_2O \rightarrow 4SO_4^{2-} + 4H^+ + O_2 \quad (3)$$

Although the rate constant has been about 87% smaller at 5.0×10^{-2} mol dm^{-3} in $UV/S_2O_8^{2-}$ (5.94×10^{-2} min^{-1}) with respect to the $UV/S_2O_8^{2-}/TiO_2$ (11.1×10^{-2} min^{-1}), a linear increase from this concentration up to 50.0×10^{-2} mol dm^{-3} (23.9×10^{-2} min^{-1}) with a slope of 1.85 mol dm^{-3} min^{-1} ($r = 0.9981$) indicates that the herbicide removal in $UV/S_2O_8^{2-}$ medium is easier than in the $UV/S_2O_8^{2-}/TiO_2$ process. Thus, the rate constant of imazapyr degradation in this process was larger in comparison to the oxidation with only persulfate ($UV/S_2O_8^{2-}$) up to 20.0×10^{-2} mol dm^{-3} $S_2O_8^{2-}$. The rate constant enhancement in the presence of TiO_2 ($UV/S_2O_8^{2-}/TiO_2$) from 2.2×10^{-2} min^{-1} at 1.0×10^{-3} mol dm^{-3} until 16.3×10^{-2} min^{-1} at 20.0×10^{-2} mol dm^{-3} $S_2O_8^{2-}$ is mainly due to the reaction with the photogenerated electron, producing sulfate radical anion (Eq. (4)).

$$S_2O_8^{2-} + e^-_{cb} \rightarrow SO_4^{\bullet -} + SO_4^{2-} \quad (4)$$

The inhibition at 50.0×10^{-2} mol dm^{-3} $S_2O_8^{2-}$ to 7.06×10^{-2} min^{-1} may be attributed to the excess of sulfate anion concentration adsorbed on the TiO_2 surface that subsequently reduces the catalytic activity and the herbicide photodegradation [8].

Consequently, imazapyr homogeneous oxidation was more favorable over the heterogeneous TiO_2-catalyzed oxidation in higher concentrations of persulfate.

The effect of addition of H_2O_2 in concentrations from 1.0×10^{-2} to 10.0×10^{-2} mol dm^{-3} at 30.0°C has been investigated and the degradation rate constants as a function of H_2O_2 in aqueous solution and in TiO_2 suspension is presented in Table 2. The oxidation capacity of H_2O_2 in aqueous imazapyr solution was not significant, because the rate constant increased from 0.41×10^{-2} to 0.59×10^{-2} min^{-1} in the range between 1.0×10^{-2} and 10.0×10^{-2} mol dm^{-3}. This effect was attributed only to direct photolysis of H_2O_2 that generated hydroxyl radicals (Eq. (5)) [1]

$$H_2O_2 + h\nu \rightarrow 2HO^{\bullet} \quad (5)$$

On the other hand, the addition of H_2O_2 in TiO_2 suspension enhanced the rate constant from 2.15×10^{-2} min^{-1} at 1.0×10^{-2} mol dm^{-3} H_2O_2 up to a maximum of 5.56×10^{-2} min^{-1} at 5.0×10^{-2} mol dm^{-3} H_2O_2, and decreased up to 1.18×10^{-2} min^{-1} at 10.0×10^{-2} mol dm^{-3}. The enhancement was attributed also to the inhibition of electron-hole recombination, producing hydroxyl radical through the reduction of H_2O_2 (Eq. (6)) and by the oxidation of the adsorbed water molecules as shown by the Eqs. (7) and (8) [1, 3–5].

$$H_2O_2 + e^-_{cb} \rightarrow HO^{\bullet} + HO^- \quad (6)$$

$$H_2O_{ads} + h^+_{vb} \rightarrow HO^{\bullet} + HO^+ \quad (7)$$

$$HO^-_{ads} + h^+_{vb} \rightarrow HO^{\bullet} \quad (8)$$

The inhibition of the electron-hole pair occurs by the formation of the superoxide radical ions (Eq. (9)) that reacts with H_2O_2 in order to produce hydroxyl radical (Eq. (10)) [1, 3–5].

$$O_2 + e^-_{cb} \rightarrow O_2^{\bullet -} \quad (9)$$

$$H_2O_2 + O_2^{\bullet -} \rightarrow HO^{\bullet} + HO^- + O_2 \quad (10)$$

At higher H_2O_2 concentrations the removal rate decreases due to the scavenging effect of the hydroxyl radical [8] by the reaction with another hydrogen peroxide molecule to yield hydroperoxyl radical, $HO_2^{\bullet}$ [1, 4]. This species is much less reactive (Eq. (11)) and can thus suppress any rate enhancement by decreasing the rate constant.

$$H_2O_2 + HO^{\bullet} \rightarrow HO_2^{\bullet} + H_2O \quad (11)$$

Effect of Temperature

The degradation rate constant was measured by varying the temperature from 20.0 to 50.0°C using a suspension of 50.0 μmol dm^{-3} imazapyr and 5.0 g dm^{-3} TiO_2 at $pH = 4.0$ under UV radiation. The rate constant increased in this range by 38% as displayed in Table 3, and the plot of the natural logarithm of the rate constant, k_{obs}, as a function of reciprocal absolute temperature did not comply well ($r = 0.9391$) with the *Arrhenius* equation.

This deviation was attributed to the combination of the desorption effects due to the temperature elevation and the TiO_2 particles agglomeration owing to the relatively large photocatalyst concentration (5.0 g dm^{-3}) in suspension. It is also relevant to point

Table 3. Rate constant, k_{obs}, of imazapyr degradation in TiO_2 suspension at $pH = 4.0$ as a function of temperature

Temperature/°C	k_{obs} $10^2/min^{-1}$
20.0	2.85
30.0	3.03
35.0	3.60
40.0	3.82
50.0	3.94

$[imazapyr]_o = 50.0\,\mu mol\,dm^{-3}$; $[TiO_2] = 5.0\,g\,dm^{-3}$

out that the temperature increase under UV radiation, may lead to the water molecules desorption due to the increase of the vapor pressure. This effect will decrease the number of water molecules available on semiconductor surface, that photogenerates the hydroxyl radical, withdrawing the collision number and consequently, the rate constant. Furthermore, the temperature increase may break the agglomerates of TiO_2 particles in a random way and lead to non-*Arrhenius* behavior. The rate constant for imazapyr degradation enhances with the temperature increase analogous to imazaquin [18], but unlike that of the imazethapyr, where the rate constant decreases with the temperature elevation [19].

Experimental

Imazapyr ($C_{13}H_{15}N_3O_3$, 93%) was kindly supplied by BASF/Brazil. P25 titanium dioxide (TiO_2) was a gift from Degussa/Brazil and was used as photocatalyst without further treatment. Acetonitrile was chromatography grade and purchased from Mallinckrodt. All other chemicals were analytical grade and used as received. The water was purified with a USF Elga Maxima system.

All the experiments were carried out in analogous conditions as reported earlier [18, 19]. The suspension was sonicated for 30 min in the dark at room temperature to attain the adsorption–desorption equilibrium between herbicide and TiO_2. Irradiations were performed under a 125 W mercury lamp (Philips, HPLN) without a bulb at 30.0 ± 0.1°C during 4 h and covered to avoid evaporation. The irradiance [$(420 \pm 19)\ \mu W\,cm^{-2}$] was measured at 365 nm and 16 cm from the lamp to the suspension surface.

The herbicide degradation was monitored at 210 nm by HPLC using a UV detector based on a diode array (Shimadzu LC-10AD, SPD M10AVP; C-18 column, 5 μm, 47×250 mm, C-18 pre-column, Metachem). A 20:80 mixture of acetonitrile-phosphate buffer (v/v) at *pH* 3.0 was used as the mobile phase at a flow rate of $1.0\,cm^3\,min^{-1}$ at 35°C and a retention time of 5.5 min. The imazapyr degradation was studied following a kinetic model of first order at 30.0 ± 0.1°C.

The charge densities of the imazapyr species, namely, protonated (imp^+), zero charge ($imp^\pm$), and deprotonated (imp^-) were calculated. The geometries were optimized at the semi-empirical AM1 level [10–23] and the *Baker* algorithm without geometry restriction [24]. The dihedral angle N3(imidazol)-C2(imidazol)-C2(pyridine)-N1(pyridine) was obtained by rotating in 15° increments between 0 and 360°.

Acknowledgements

The authors gratefully acknowledge the financial support of CNPq and CAPES. We also thank CAPES for a fellowship to *JAO*.

References

[1] Legrini O, Oliveros E, Braun AM (1993) Chem Rev **93**: 671
[2] Hoffmann MR, Martin SC, Choi W, Bahnemann DW (1995) Chem Rev **95**: 69
[3] Malato S, Blanco J, Richter C, Braun B, Maldonado MI (1998) Appl Catal B **17**: 347
[4] Wang Y, Hong C (1999) Water Res **33**: 2031
[5] Neppolian B, Choi HC, Sakthivel S, Arabindoo B, Murugesan V (2002) Chemosphere **46**: 1173
[6] Mills A, Valenzuela MA (2004) J Photochem Photobiol A **165**: 25
[7] Lee C, Yoon J (2004) J Photochem Photobiol A **165**: 35
[8] Muruganandham M, Swaminathan M (2004) Solar En Mater Solar Cells **81**: 439
[9] Cox C (1996) J Pestic Reform **16**: 16
[10] Pizarro P, Guillard C, Perol N, Herrmann J-M (2005) Catal Today **101**: 211
[11] Carrier M, Perol N, Herrmann J-M, Bordes C, Horikoshi S, Paisse JO, Baudot R, Guillard C (2006) Appl Catal B **65**: 11
[12] Fujishima A, Rao TN, Tryk DA (2000) J Photochem Photobiol C **1**: 1
[13] Konstantinou IK, Albanis TA (2004) Appl Catal B **49**: 1
[14] Augugliaro V, Litter M, Palmisano L, Soria J (2006) J Photochem Photobiol C **7**: 127
[15] O'Neil MJ, Smith A, Heckelman PE (eds) (2001) The Merck Index, 13th edn. Merck, White House Station, p 880
[16] Schindler PW, Gamsjäger H (1972) Kolloid-Z u Z Polymere **250**: 759
[17] O'Shea KE, Cardona C (1995) J Photochem Photobiol A **91**: 67
[18] Garcia JC, Takashima K (2003) J Photochem Photobiol A **155**: 215
[19] Ishiki RR, Ishiki HM, Takashima K (2005) Chemosphere **58**: 1461
[20] Dewar MJS, Zoebisch EG, Healy EF, Stewart JJP (1985) J Am Chem Soc **107**: 3902
[21] Dewar MJS, Yuan YC (1990) Inorg Chem **29**: 3881
[22] Dewar MJS, Zoebisch EG (1998) J Mol Struct (Theochem) **49**: 1
[23] Stewart JJP (1993) MOP AC 93 Manual, Fujitsu, Tokyo
[24] Baker J (1986) J Comput Chem **7**: 385